BIODIVERSITAS
Volume 24, Number 5, May 2023
Pages: 2689-2700

ISSN: 1412-033X
E-ISSN: 2085-4722
DOI: 10.13057/biodiv/d240522

Analysis of the effect of ENSO and IOD on the productivity of yellowfin tuna (*Thunnus albacares*) in the South Indian Ocean, East Java, Indonesia

ABU BAKAR SAMBAH[1,2,♥], AURUM NOOR'IZZAH[1], CANDRA ADI INTYAS[3], DENNY WIDHIYANURIYAWAN[4], DIDIED POERNAWAN AFFANDY[5], ADI WIJAYA[6]

[1]Department of Fisheries and Marine Sciences, Faculty of Fisheries and Marine Sciences, Universitas Brawijaya. Jl. Veteran, Malang 65145, East Java, Indonesia. Tel.: +62-341-553512, Fax.: +62-341-557837, ♥email: absambah@ub.ac.id

[2]Marine Resources Exploration and Management Research Group, Faculty of Fisheries and Marine Sciences, Universitas Brawijaya. Jl. Veteran, Malang 65145, East Java, Indonesia

[3]Department of Fisheries and Marine Socio-Economic, Faculty of Fisheries and Marine Sciences, Universitas Brawijaya. Jl. Veteran, Malang 65145, East Java, Indonesia

[4]Department of Mechanical Engineering, Faculty of Engineering, Universitas Brawijaya. Jl. MT. Haryono 167, Malang 65145, East Java, Indonesia

[5]Department of Accounting, Faculty of Economic and Business, Universitas Brawijaya. Jl. MT. Haryono 165, Malang 65145, East Java, Indonesia

[6]Institute for Marine Research and Observation, Ministry of Marine Affair and Fisheries. Jl. Baru, Perancak, Negara, Jembrana 82218, Bali, Indonesia

Manuscript received: 20 November 2022. Revision accepted: 16 May 2023.

Abstract. *Sambah AB, Noor'izzah A, Intyas CA, Widhiyanuriyawan D, Affandy DP, Wijaya A. 2023. Analysis of the effect of ENSO and IOD on the productivity of yellowfin tuna* (Thunnus albacares) *in the South Indian Ocean, East Java, Indonesia. Biodiversitas 24: 2689-2700.* Yellowfin tuna (*Thunnus albacares*) is one of the fish that migrates through the Indian Ocean and is primarily caught in the south Java waters which are directly adjacent to the Indian Ocean. Fish abundance and migration are influenced by oceanographic factors, including climatic factors which affect annual and interannual variations, such as the Indian Ocean Dipole (IOD) and the El Nino Southern Oscillation (ENSO). This study aimed to determine the effect of climate anomalies on the productivity of yellowfin tuna in the Indian Ocean south of East Java, Indonesia. Data collection was carried out at Coastal Fishing Port of Pondokdadap East Java, involving 58 respondents consisting of fishermen with yellowfin tuna catches. The boundaries of the research area are at coordinates 110.9°-114.5° East Longitude and 8°-11° South Latitude. The data used in the analysis consisted of Sea Surface Temperature (SST) data, chlorophyll-a data, Nino 3.4 data, Dipole Mode Index (DMI) data, and yellowfin tuna catch data for the year 2017-2021. The results showed that of the fifteen GAM models, the combination of variables that most affected fish productivity was the distribution of chlorophyll-a and the ENSO phenomenon with values of AIC (1503.33) and DE (64.30%). Pearson correlation analysis showed that the IOD phenomenon was influenced by SST and chlorophyll-a, while SST and chlorophyll-a did not significantly influence the ENSO phenomenon. These results indicated that the phenomenon of climate anomalies and the oceanographic conditions in the waters indirectly affect fish productivity through the food chain process.

Keywords: ENSO, Indian ocean, IOD, oceanographic factors, yellowfin tuna

INTRODUCTION

The southern waters of Java are directly adjacent to the Indian Ocean and characterized by large waves, sandy substrate and steep seabed topography. Oceanographic dynamics in the southern waters of Java are affected by several factors such as the Indian Ocean Dipole (IOD) phenomenon, El Nino Southern Oscillation (ENSO), Indonesia Through Flow (ITF), and Kelvin waves, in which the phenomenon IOD + describe the most influence to the decreasing of sea level anomaly (Fadlan et al. 2017). Both the spatial and temporal patterns of the ocean and atmospheric variability affect the dynamics of marine waters in Indonesia, this includes the phenomena related with the monsoonal system; Indonesia Through Flow (ITF), El Nino-Southern Oscillation (ENSO), Indian Ocean Dipole (IOD), and Madden Julian Oscillation (MJO) (Wijaya et al. 2020). As a result of this phenomenon, the surface layer of primary productivity experiences variations due to the Australian to Asian monsoon system. The ENSO and the IOD have been known to induce variability in ocean surface characteristics along the Indonesian waters. The upwelling phenomenon is caused not only by the southeast monsoon season but also by the ENSO and IOD (Simanjuntak and Lin 2022).

Monsoon and ENSO variations are closely related to the annual and interannual variations of the ITF, where during the southeast monsoon the ITF tends to be higher than during the northeast monsoon (Sprintall and Revelard 2014). ENSO is a naturally occurring phenomenon involving fluctuating ocean temperatures in the central and eastern equatorial Pacific, coupled with changes in the atmosphere (Nur'utami and Hidayat 2016; Lau and Yang 2022). ENSO can be described as periodic fluctuation (i.e., every 2-7 years) in Sea Surface Temperature/SST (El Niño) and the air pressure of the overlying atmosphere (Southern Oscillation) across the equatorial Pacific Ocean. The term oscillation illustrated the shifting between El Niño and La Niña conditions occurring every few years (Bjerknes 1966;

Santoso et al. 2017; Wang et al. 2017; Lee et al. 2022). The type of ENSO could affect the dynamics of marine fisheries, including the distribution of fish habitat and the potential fishing grounds, as well as the composition of fish catch. This can have impact on some fish populations in the Atlantic Ocean and tuna fisheries in the Indian Ocean. Further analysis of fish populations and sizes could shed light on longer-term effects of ENSO events, as they can alter habitats and marine food webs long after they have ended.

The IOD phenomenon is a result of the interaction of the ocean and atmosphere in the tropical Indian Ocean, and it has a significant impact on the Indian Ocean region (Yang et al. 2019). Oceanographic factors, sea surface temperature and the concentration of chlorophyl-a are important factors in estimating potential fishing grounds, especially for pelagic fish. Furthermore, global phenomena such as IOD and ENSO have an indirect influence on the dynamics of aquatic environmental parameters. Different types of positive IOD occurrences result in varying ocean circulation responses, resulting in varying patterns in chl-a anomalies in the Indian Ocean (Sari et al. 2020; Simanjuntak and Lin 2022). The high and low catch of *Sardinella lemuru* (Bleeker, 1853) in the Bali Strait are affected by the IOD and ENSO phenomena (Sambah et al. 2013).

The Indian Ocean region includes the Fisheries Management Area of Republic of Indonesia (FMA-RI 573) in the southern part of Java Island, a migration area for large pelagic fish such as tuna species, and habitat for demersal fish. Bigeye tuna (*Thunnus obesus* Lowe, 1839), yellowfin tuna (*Thunnus albacares* Bonnaterre, 1788), albakor (*Thunnus alalunga* Bonnaterre, 1788), and skipjack tuna (*Katsuwonus pelamis* Linnaeus, 1758) are the four fish species that are mostly caught in FMA-RI 573 (Harlyan et al. 2020). The distribution of tuna species as well as other pelagic fish are closely related to the oceanographic factors. Various studies related to the effect of El Nino Southern Oscillation and Indian Ocean Dipole on fish caught have been previously carried out by Setyadji and Amri (2017) on the distribution of swordfish (*Xiphias gladius* Linnaeus, 1758) in the eastern Indian Ocean, Wijaya et al. (2020) on the resources of lemuru fish (*S. lemuru*) in the Bali Strait, Syamsuddin et al. (2013), Lumban-Gaol et al. (2015), and Hsu et al. (2021) on bigeye tuna (*T. obesus*) in the Indian Ocean south of Java (Amri and Satria 2013) on the composition of catches of neritic tuna in the Sunda Strait. In this study, the dynamic of yellowfin tuna is a variable to be studied together with the effect of climate anomalies and oceanographic factors included SST and chlorophyll-a related to the productivity and sustainability of yellowfin tuna (*T. albacares*) in the Indian Ocean south of East Java on their habitats.

MATERIALS AND METHODS

Study area

This research was a quantitative descriptive study where primary data was obtained by participatory mapping method in direct interviews with 58 fishermen at the Coastal Fishery Port (CFP) of Pondokdadap, Malang District, East Java, Indonesia who caught yellowfin tuna (*T. albacares*) in the southern Indian Ocean region of East Java. The result of the interview was the point of the fishing ground (geographical coordinates) where the fishing gear was set. Interviews were conducted with fishermen in this study using a sampling technique. Sampling in the study was determined by purposive sampling technique.

The secondary data used consisted of SST data, chlorophyll-a data, Nino 3.4 data, Dipole Mode Index (DMI) data, and yellowfin tuna (*T. albacares*) catch data. Nino 3.4 data is an index of the ENSO phenomenon, while DMI data is an index of the IOD phenomenon. SST data, chlorophyll-a data, nino 3.4 data, DMI data, and catch data of yellowfin tuna (*T. albacares*) were processed in the last five years. SST and chlorophyll-a data were obtained through the website https://oceancolor.gsfc.nasa.gov. Nino 3.4 data and DMI data are obtained from the website https://psl.noaa.gov/gcos_wgsp/Timeseries/Data/. The coordinates of the fishing area and data on the catch of yellowfin tuna (*T. albacares*) in 2017-2021 were obtained from the data from the CFP Pondokdadap fisheries statistical report. Coordinates of fishing areas from fisheries statistics data or CFP Pondokdadap logbook and interviews with fishermen who were involved in catching yellowfin tuna (*T. albacares*) were used as the boundaries of the research area (110.9°-114.5° East Longitude, 8°-11° South Latitude), as shown in Figure 1.

Procedures and data analysis

In this study, the Nino 3.4 index was used as the ENSO index, while the DMI value was used for the IOD phenomenon. The Nino index of 3.4 can represent the average SST in the equatorial region. The ENSO prediction approach using the Nino 3.4 SST anomaly index has represented the ENSO phenomenon. This approach is relatively lower in real-time forecasts than in hindcasts and varies during epochs with considerable uncertainties (Barnston et al. 2012; Ren et al. 2017; Ren et al. 2019). Furthermore, the DMI value in this study was used as an indicator that shows the occurrence of the IOD phenomenon, both IOD+ and IOD-. DMI value data can be downloaded through the official NOAA website, representing the difference in SST anomaly values between the Western Indian Ocean and the Eastern Indian Ocean. The information on fishing ground coordinate was collected through direct interview with the longline fishermen. This information includes primary data and description of the geographic points of the fishing gear set during fishing operation. Moreover, the fishing ground logbook as the secondary data were also applied to validate the distribution of the fishing ground the research area.

The relationship of SST and chlorophyll-a every month during 2017-2021 to the El Nino Southern Oscillation index value (Nino 3.4) and the IOD index value DMI, were analyzed using Pearson correlation analysis. Meanwhile, the effect of SST, chlorophyll-a, ENSO and IOD on yellowfin tuna, with a case study of data collection at CFP Pondokdadap and research boundaries 110.9°-114.5° east and 8°-11° south latitude analyzed by GAM analysis using package ‘gam’ version 1.22-2 in the the R-studio application. The research procedure is described in Figure 2.

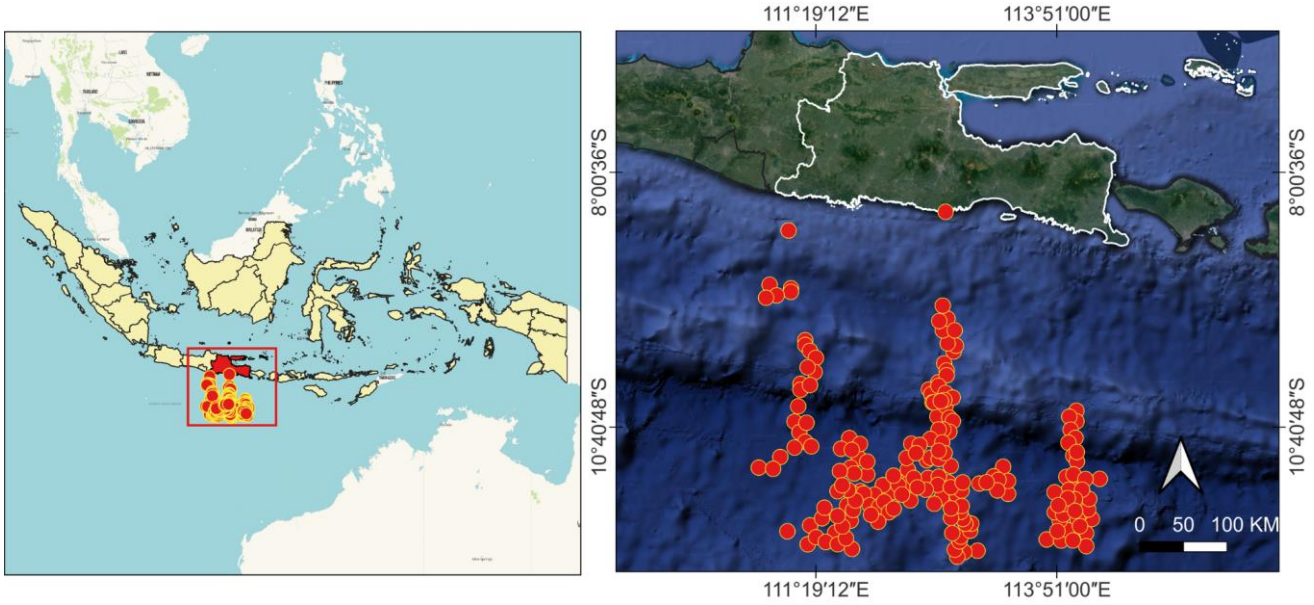

Figure 1. Map of research location

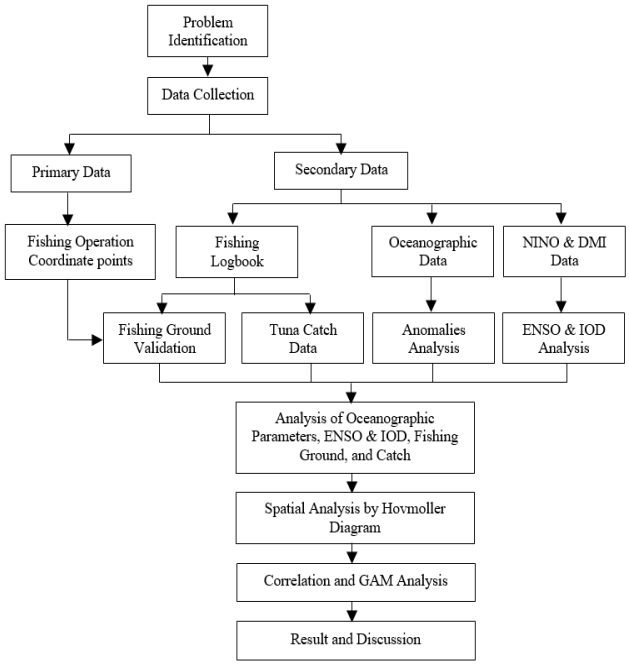

Figure 2. Research flowchart

RESULTS AND DISCUSSION

Yellowfin tuna catch production

The total volume of yellowfin tuna production at CFP Pondokdadap showed an increasing trend (Figure 3). The largest total volume of yellowfin tuna production in CFP Pondokdadap was recorded at 1,720,859 kg in 2021, to be precise in July, reaching 394,404 kg (Figure 4). Meanwhile, the smallest total production volume at CFP Pondokdadap was 981,278 kg in 2020. The catch of yellowfin tuna in CFP Pondokdadap has a high average catch in May - July. Meanwhile, in the western season, namely in December - February, the catch of yellowfin tuna decreases.

ENSO and IOD phenomena

The Nino index 3.4 can show El Nino and La Nina phenomena with values based on the index classification (Table 1) in six months or more in a row (Saputra et al. 2017).

The DMI index can be classified if the DMI index value is > 0.35, it indicates the IOD+ phenomenon. On the other hand, when the DMI index value is <-0.35, it can be categorized as the IOD- phenomenon. When the index value between -0.35 to 0.35 occurs when the phenomenon is normal/neutral IOD. The DMI index can show the IOD phenomenon when it lasts for 3 months or more for a year in a row (Thushara and Vinayachandran 2020). The results of the study obtained through Nino 3.4 index and the DMI index during the years 2017-2021 showed two La Nina phenomena, one El Nino phenomenon, and three IOD+ phenomena.

In 2017-2021, a weak La Nina phenomenon was found in 2017-2018, an El Nino phenomenon in 2018-2019, and a weak La Nina phenomenon in 2020-2021. The weak La Nina phenomenon in 2017-2018 lasted for 7 years, month from September-March (Figure 5A). The El Nino phenomenon in 2018-2019 lasted 9 months, from October to June (Figure 5B). The weak La Nina phenomenon in 2020-2021 lasted 8 months, from September to April (Figure 5C).

In 2017-2021, the IOD+ phenomenon was discovered in 2017, the IOD+ phenomenon at the end of 2018 to the beginning of 2019, and the IOD+ phenomenon in mid-2019. In 2017, the IOD+ phenomenon lasted for 6 months from March to August (Figure 6A). From the end of 2018 to the beginning of 2019, the IOD+ phenomenon lasted 6 months from September to February (Figure 6B). In mid-2019, IOD+ lasted 7 months, from May to November (Figure 6C). In 2019, two IOD+ phases were discovered for one year.

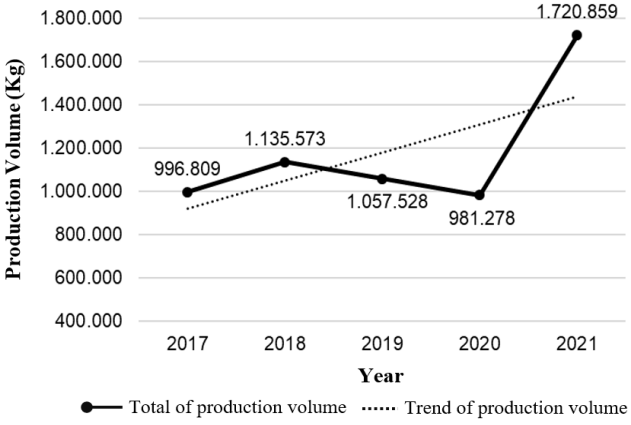

Figure 3. The trend of yellowfin tuna production at CFP Pondokdadap, Malang District, East Java, Indonesia

Table 1. The Nino 3.4 Index

Nino 3.4 SST anomaly index (°C)	Phenomena
>2.0	Strong *El Nino*
1.0 – 2.0	Moderate *El Nino*
0.5 – 1.0	Weak *El Nino*
-0.5 – 0.5	Neutral/Normal
-1.0 – -0.5	Weak *La Nina*
-2.0 – -1.0	Moderate *La Nina*
<-2.0	Strong *La Nina*

Source: NOAA ESRL Physical Sciences Laboratory (2018)

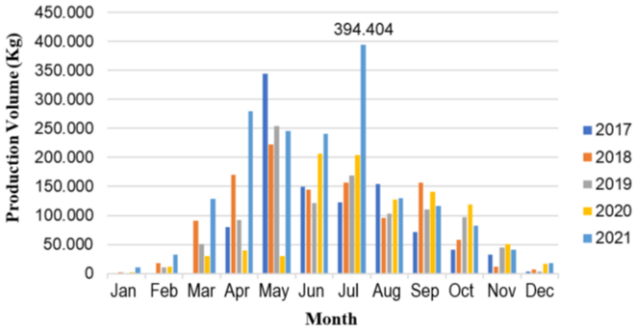

Figure 4. Monthly production of yellowfin tuna at CFP Pondokdadap, Malang District, East Java, Indonesia

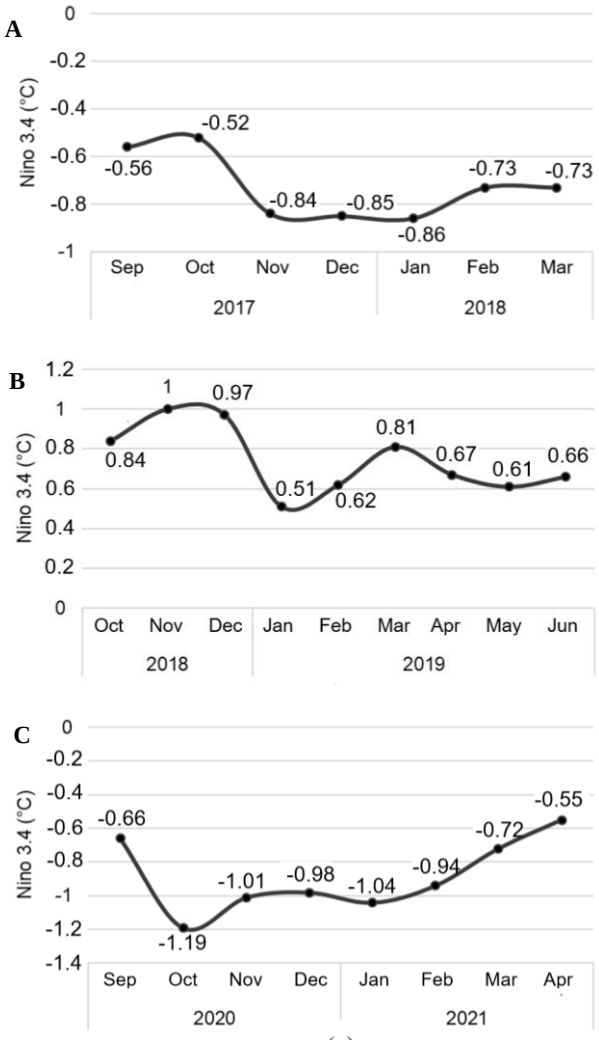

Figure 5. Nino 3.4 Fluctuations during the ENSO Phenomenon: A. La Nina phenomenon, B. El Nino phenomenon, C. La Nina phenomenon

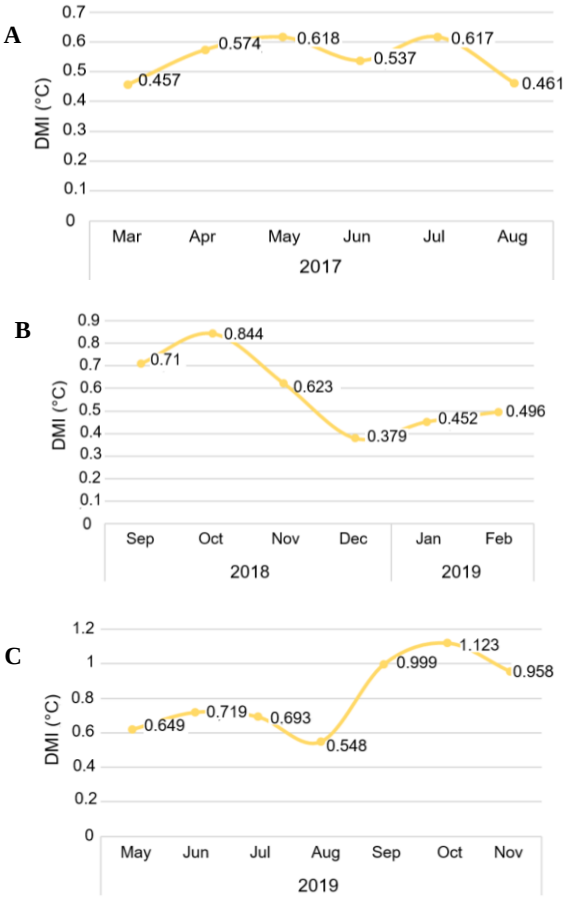

Figure 6. DMI Fluctuations during the IOD Phenomenon: A. IOD+ phenomenon, B. IOD+ phenomenon, C. IOD+ phenomenon

Variability of sea surface temperature and chlorophyll-a and their relationship with ENSO and IOD phenomena

The average SST in the southern waters of East Java in 2017-2021 ranged from 25.06°C to 30.62°C. SST in the southern waters of East Java tend to be low in the east monsoon (Figure 7). The average chlorophyll-a in the southern waters of East Java at 2017-2021 ranged from 0.09 mg/m^3 to 0.92 mg/m^3. Chlorophyll-a in the southern waters of East Java tend to be high in the east monsoon (Figure 8).

The relationship between SST and chlorophyll-a per month on the El Nino Southern Oscillation index value (Nino 3.4) and DMI as an IOD index was analyzed using Pearson correlation analysis. The results of the Pearson correlation analysis (Table 2) show that the average SST has a significant effect on chlorophyll-a (0.000 < 0.05), but the average SST has no significant effect on the value of the Nino index 3.4 (0.655 > 0.05). The average value of chlorophyll-a concentration also had no significant effect on the value of Nino 3.4 (0.328 > 0.05).

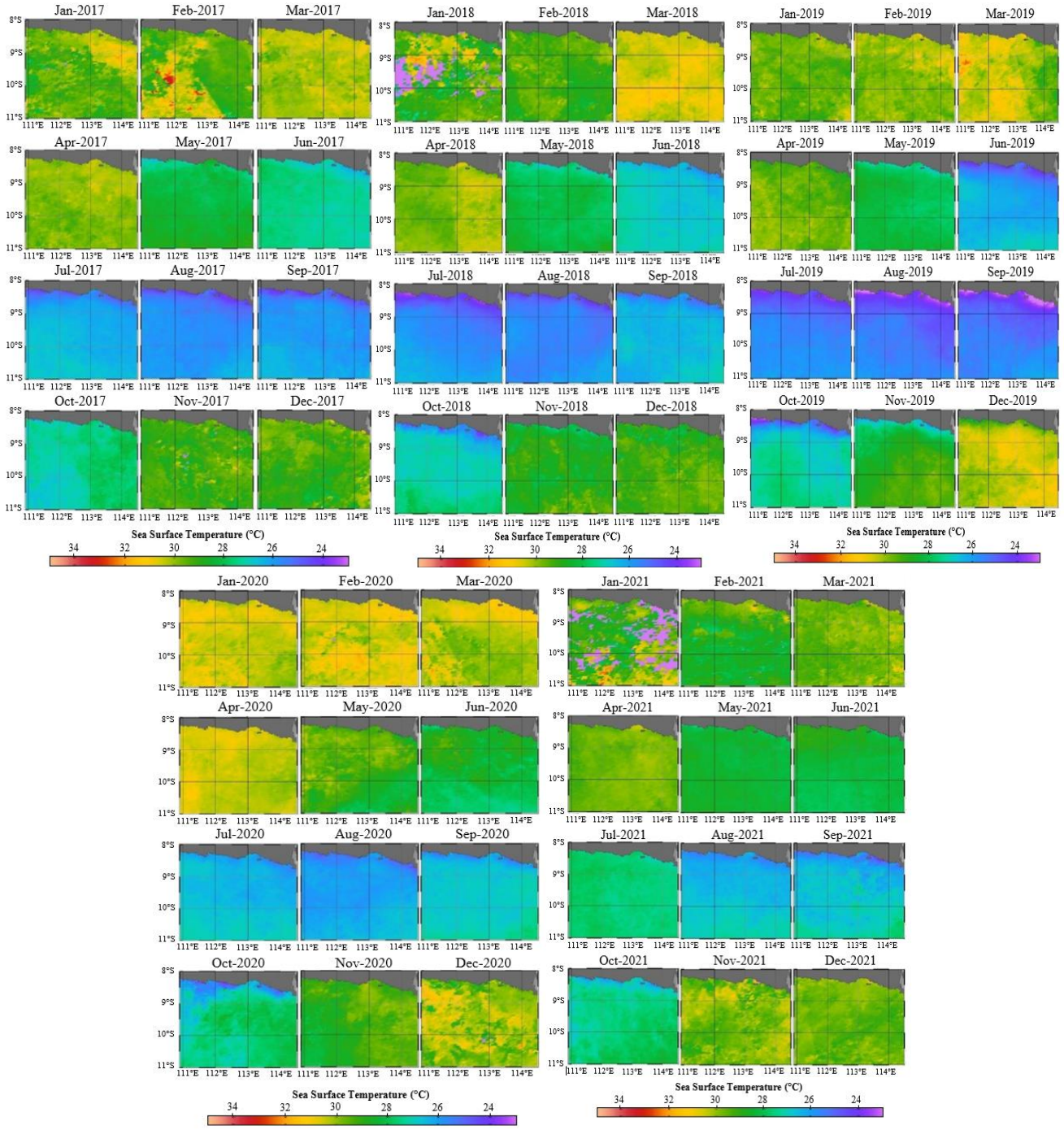

Figure 7. Distribution of SST (°C) in Southern Waters of East Java, Indonesia for 2017, 2018, 2019, 2020, and 2021

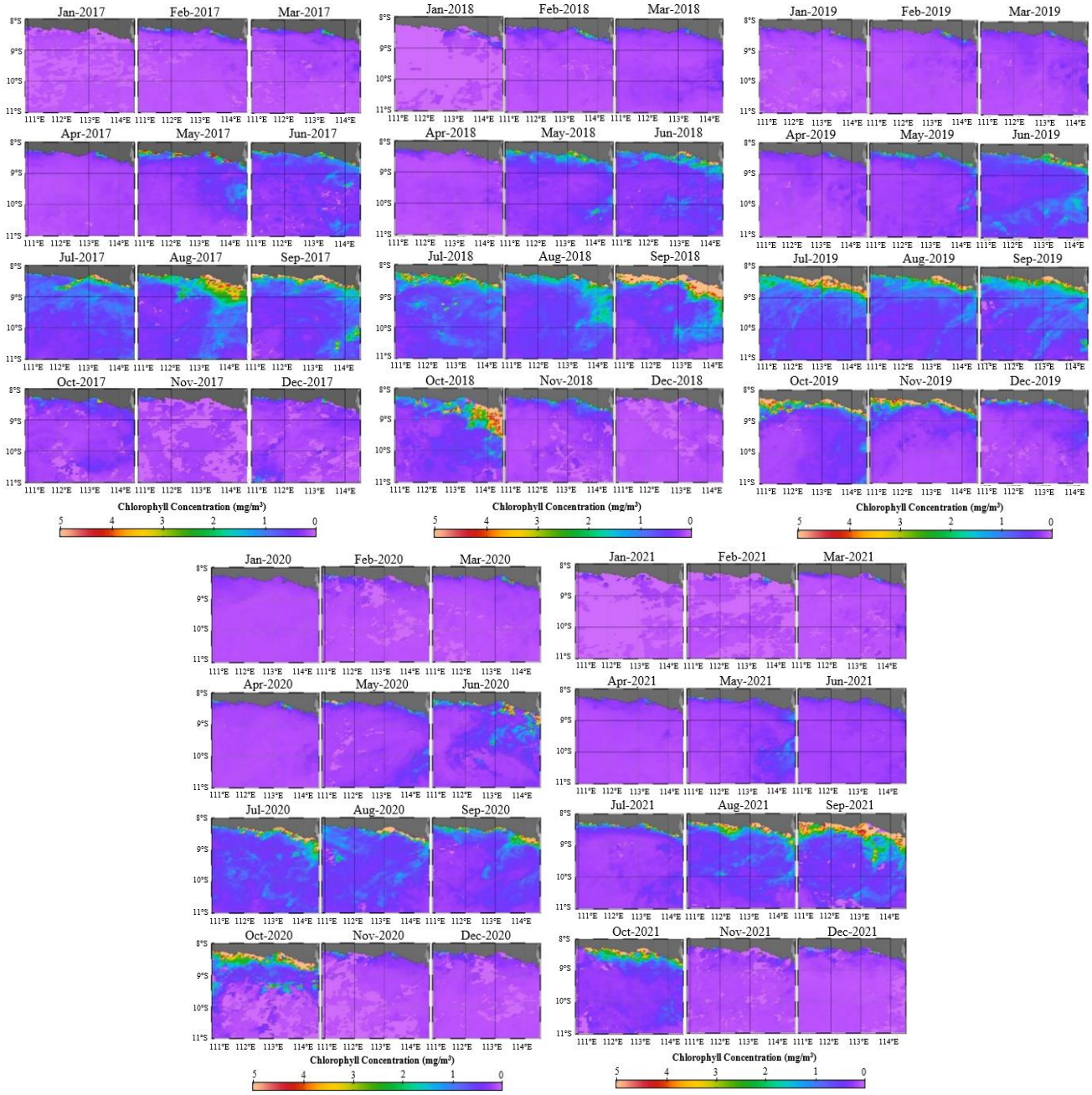

Figure 8. Distribution of chlorophyll-a (mg/m^3) in the Southern Waters of East Java, Indonesia for 2017, 2018, 2019, 2020, and 2021

Table 2. Correlation of SST and Chlorophyll-a to ENSO and IOD phenomena

	SST	Chlorophyll-a	DMI	NINO 3.4
SST	1	-0.926**	-0.289*	-0.059
Chlorophyll-a	-0.926**	1	0.319*	0.128
DMI	-0.289*	0.319*	1	0.571**
NINO 3.4	-0.059	0.128	0.571**	1

Note: **. Correlation is significant at the 0.01 level (2-tailed), *. Correlation is significant at the 0.05 level (2-tailed)

The results of the Pearson correlation analysis (Table 2) show that SST has a significant effect on the DMI value (0.025 < 0.05). The relationship between SST and DMI value is inversely proportional to the Pearson correlation test value of -0.289. The correlation value between SST and DMI shows a low level of relationship. The chlorophyll-a variable also significantly affected the DMI value (0.013 < 0.05). The relationship between chlorophyll-a and DMI values is directly proportional to the Pearson correlation test value of 0.329.

The Hovmoller diagram (Figure 9) shows the anomaly values of SST and chlorophyll-a for the El Nino Southern Oscillation phenomenon that occurred during 2017-2021. When the La Nina phenomenon occurred in 2017-2018, in 2020-2021, and at the end of 2021 showed SST anomalies

ranging from -2°C to 3.5°C and chlorophyll-a anomaly values ranging from > -0.5 mg/m^3 to 5 mg/m^3. Meanwhile, the El Nino phenomenon that occurred at the end of 2018 to mid-2019 and at the end of 2019 to early 2020 showed SST anomalies ranging from -4 to 2.5 and chlorophyll-a anomaly values ranging from -0.5 to > 5. When the El Nino phenomenon occurs, the anomaly value tend to be positive. On the contrary, when the La Nina phenomenon occurs, the anomaly tend to have a negative value (Wijaya et al. 2020). In the south waters of Java, the anomaly value in December - February tend to increase (Santoso et al. 2021).

The Hovmoller diagram (Figure 10) shows the SST and chlorophyll-a anomaly values for the IOD phenomenon that occurred during 2017-2021. When the IOD+ phenomenon occurred in 2017, late 2018 to early 2019, middle-2019 and 2020, water conditions showed SST anomalies ranging from -4°C to 1.5°C and chlorophyll-a anomaly values ranging from -0.5 mg/m^3 to > 5 mg/m^3. Based on the Hovmoller diagram, the abnormal values of SST and chlorophyll-a are inversely proportional. When the value of the chlorophyll-a anomaly is high, on the other hand, the value of the SST anomaly is low. IOD+ tend to affect the increase in chlorophyll-a so that the chlorophyll-a anomaly can reach 1 mg/m^3 to > 4.5 mg/m^3. In the southern coastal waters of Java, the average chlorophyll-a anomaly value ranges from 5 mg/m^3 to > 12 mg/m^3 (Santoso et al. 2021).

Moreover, catch fluctuations and the El Nino Southern Oscillation index, namely Nino 3.4 (Figure 10A) show that when a weak La Nina phenomenon occurred in 2017-2018 for a period of 7 months (September-March) the catch of yellowfin tuna decreased with an average yield catch of 36,987 Kg. In the weak El Nino phenomenon from the end of 2018 to the middle of 2019 for 9 months (October-June), the average catch increased by 67,316 Kg. Then the weak La Nina phenomenon in 2020-2021 for 8 months (September-April) shows an increasing catch with an average catch of 97,379 Kg. Fluctuations in the Nino 3.4 index are seen to follow changes in the catch of yellowfin tuna (*T. albacares*). The fluctuation of catch and the Indian Ocean Dipole index, namely DMI (Figure 11B) shows that when the IOD+ phenomenon occurred in 2017 for a period of 6 months (March-August) the average yellowfin tuna catch was 141,523 Kg. In the IOD+ phenomenon from the end of 2018 to the beginning of 2019 for 6 months (September-February), the fish catch showed an average of 40,892 Kg. The IOD+ phenomenon in mid-2019 for a 7-month period (May-November) showed an average catch of 128,708 Kg. DMI index fluctuations are not directly proportional to fluctuations in the catch of yellowfin tuna (*T. albacares*). The relationship between ENSO and skipjack fishing can be used as evidence for predictions of fishing areas two months in advance. ENSO indices such as SST variation, and the Southern Oscillation Index (SOI) can also be predicted by statistical models to look at the annual dynamics of the ocean-atmosphere model. The applications of dynamic-coupled, statistical, and data-driven models in ENSO prediction have focused on predicting ENSO indices (e.g., Nino 3.4) (Lee et al. 2022).

Generalized additive model analysis

From the generalized additive model analysis fifteen models were obtained from the combination of 4 tested variables: SST, chlorophyll-a, Nino 3.4 as the ENSO index, and DMI as the IOD index. Of all the models (Table 3), only model no. 1 (SST), model 2 (chlorophyll-a), model 3 (Nino 3.4), and model 8 (chlorophyll-a + Nino 3.4) had a significant effect on fish catches (p-value < 0.001 or p-value < 0.005). Among the models, model 1 (SST), model 2 (chlorophyll-a), model 3 (Nino 3.4), and model 8 (chlorophyll-a + Nino 3.4), criteria of the lowest values of AIC and highest DE was met by model 8 (AIC = 1503.33 and DE = 64.30%). The evaluation of the models took into account the significance level of predictors (P-value), the amount of Deviance Explained (DE), and the Akaike Information Criterion (AIC) value. The best model was determined based on the lowest AIC value and the highest DE. The lower AIC value indicates higher significance (Mugo et al. 2010; Setiawati et al. 2015).

The Generalized Additive Model (GAM) plot (Figure 11) shows the relationship between each predictor variable to the response variable. In the SST variable, it can be seen that the productivity of yellowfin tuna tend to increase in the temperature range of 27°C-28.5°C. The chlorophyll-a variable shows that the productivity of yellowfin tuna has a high chance with chlorophyll-a concentrations ranging from 0.25 mg/m^3-0.5 mg/m^3. The Nino 3.4 variable shows that the productivity of yellowfin tuna tend to increase by -0.5°C-0.5°C. Meanwhile, the DMI variable shows that the productivity of yellowfin tuna tend to increase in the range of < 0.0°C and 0.4°C-1°C. Yellowfin tuna productivity tend to decrease along with SST variable > 28.5°C, chlorophyll-a variable > 0.25 mg/m^3, Nino 3.4 < -0.5°C and > 0.5°C variable, and variable DMI 0.0°C - 0.4°C.

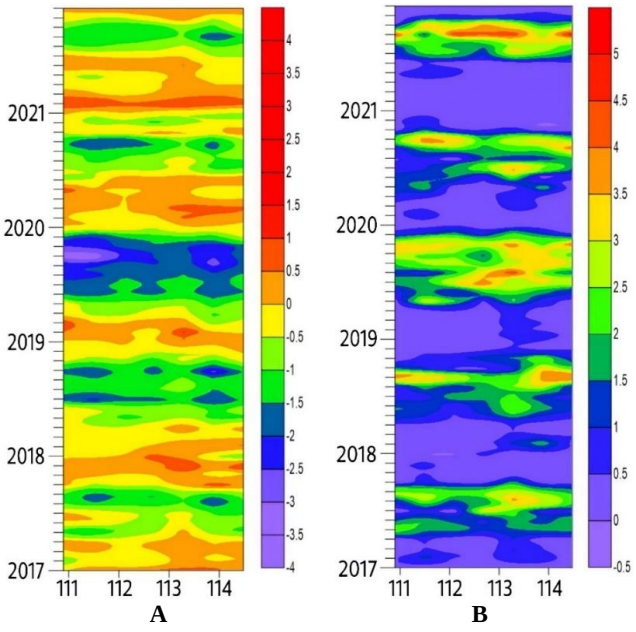

Figure 9. Hovmoller Diagram: A. SST Anomaly (°C); B. Chlorophyll-a Anomaly (mg/m^3)

Table 3. Results of GAM analysis

Model	Variable	*P-value*	DE	AIC	edf
SST	SST	8.81e-07 ***	58.8%	1505.95	7.837
Chlorophyll-a	chlorophyll-a	4.14e-05 ***	50.10%	1518.004	8.113
Nino 3.4	Nino 3.4	0.00957 **	21.60%	1533.86	2.460
DMI	DMI	0.45	7.38%	1544.39	2.737
SST + chlorophyll-a	SST	4.24e-06 ***	62%	1503.91	8.204
	chlorophyll-a	0.872			1.000
SST + Nino 3.4	SST	1.98e-06 ***	63.50%	1502.21	7.883
	Nino 3.4	0.341			1.672
SST + DMI	SST	7.35e-07 ***	67%	1501.52	8.174
	DMI	0.425			4.075
chlorophyll-a + Nino 3.4	chlorophyll-a	6.96e-06 ***	64.30%	1503.33	8.511
	Nino 3.4	0.0326 *			2.296
chlorophyll-a + DMI	chlorophyll-a	2.14e-06 ***	57.90%	1510.30	8.354
	DMI	0.101			1.000
Nino 3.4 + DMI	Nino 3.4	0.00842 **	29.30%	1533.72	2.472
	DMI	0.38306			3.013
SST + chlorophyll-a + Nino 3.4	SST	2.06e-05 ***	63.50%	1504.1	7.816
	chlorophyll-a	0.775			1.000
	Nino 3.4	0.331			1.683
SST + chlorophyll-a + DMI	SST	6.71e-06 ***	67%	1503.34	8.112
	chlorophyll-a	0.695			1.000
	DMI	0.418			4.060
SST + Nino 3.4 + DMI	SST	5.91e-06 ***	73.30%	1498.40	7.906
	Nino 3.4	0.258			1.771
	DMI	0.294			7.403
chlorophyll-a + Nino 3.4 + DMI	chlorophyll-a	1.1e-05 ***	64.20%	1505.26	8.480
	Nino 3.4	0.101			2.225
	DMI	0.596			1.000
SST + chlorophyll-a + Nino 3.4 + DMI	SST	4.05e-05 ***	72.90%	1500.52	7.804
	chlorophyll-a	0.668			1.000
	Nino 3.4	0.276			1.762
	DMI	0.341			7.162

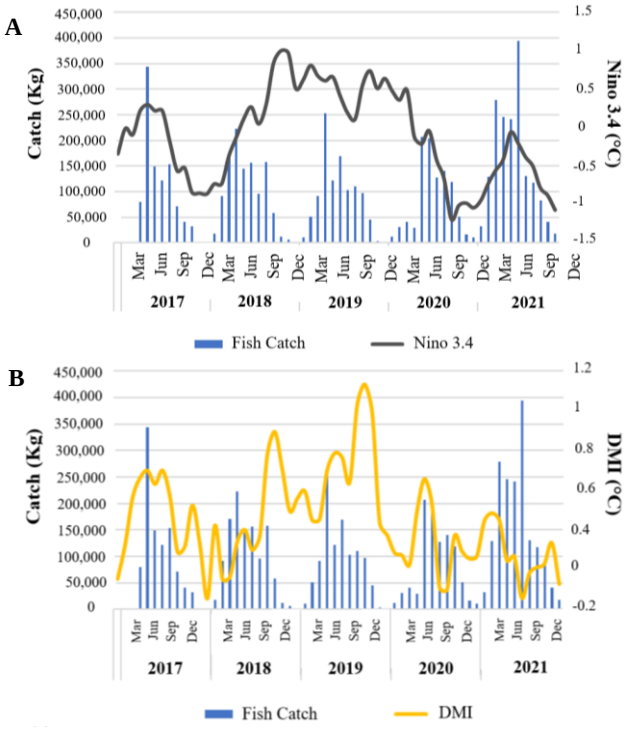

Figure 10. Climate anomaly phenomena on yellowfin tuna catches: A. ENSO phenomenon on yellowfin tuna catches, B. IOD phenomenon on yellowfin tuna catches

Discussion

The increase and decrease in fish catch recorded in the fisheries statistical data of CFP Pondokdadap cannot be separated from the influence of oceanographic parameters in the sea. Understanding the relationship between oceanographic parameters and its impact on fish distribution is essential in accurately gauging the effects of climate change globally upon fisheries resources of interest. However, this study has remained largely elusive given the lack of synoptic-level datasets on the oceanographic parameters that differentiate diverse ocean sites from each other (George et al. 2019). Satellite remote sensing technique has played an important role in addressing this data gap by offering the opportunity to observe multiple oceanographic parameters systematically at desired resolutions (George 2014). Remote sensing emerges as a very effective approach to observe the dynamics of the coastal system, as it provides a holist view of the system at a wide range of spatial and temporal scales. With the advent of satellite remote sensing capabilities, spatial and temporal changes in physical forcing and optical responses of coastal waters can easily be monitored (Lira and Taborda 2014; Kratzer et al. 2016). For example, the South East Arabian Sea reportedly exhibits a strong seasonality in remote sensing reflectance compared with its North East counterpart (Monolisha et al.

2018). Wijaya et al. (2020) also applied remote sensing approaches to investigate the inter-annual system of Bali Strait Indonesia related to the oceanographic parameter and described that Bali Strait is influenced by seasonal and inter-annual systems, where ENSO and IOD are climate changes that affect ocean conditions.

Currently, fisheries and the marine ecosystems are conceptualized as complex systems where the interaction among environmental variation (including oceanographic factors), human interventions, and the dynamics of marine populations manifest in a variety of behaviors, encompassing endless fluctuations that eventually lead to regime shifts and even fisheries collapse. The availability of long time-series of catch statistics (Peck et al. 2012; Zhang et al. 2021), catch reconstructions (Pauly and Zeller 2016), the use of satellite remote sensing for observing the ocean (George 2014), and compilations of the output of quantitative stock assessments (Cadrin and Dickey-Collas 2014), has allowed the examination of the relative incidence of distinct patterns of variability in fisheries (Peck et al. 2013).

Fish migration paths, fishing season patterns, and the number of hooks used in fishing gear also affect the catch, and fish stock management should be based on a more comprehensive understanding of population movements and behaviors across their broad distribution ranges (Aranda et al. 2013). Migration of animals, including fish in large groups, is closely related to seasonal patterns and specific geographic locations. The target locations for this migration are related to spawning and foraging areas. Migration will continue until they reach their target. In the interest of migration for spawning, the intended location for a certain period is adjusted to the reproductive cycle and its survival or growth (Fonteneau and Pereira 2012). Migration of several fish species is also affected by changes in oceanographic factors.

Based on the fishing season with the target of yellowfin tuna, the low season of catch was from December to February. Meanwhile, the peak season was from June to September. Fishing season is often used for estimating the distribution of fishing ground. In the five years data analysis, the lowest SST was found in August with an average SST of 25.78°C. Then the SST increased from the end of the transition season 2, the western season, until the beginning of the transition season 1. The highest annual average SST was in March with a value of 30.21°C. From December to February (west season) to March to May (transition season 1) the average SST in the southern region of Java tends to be high. SST in this area tend to be low in June to August (east season) and September to November (transition season 2) (Novitasari et al. 2022). The study of SST in the East China Sea described that the SST increased offshore from north to south with a range of ~8 to 25°C, and the highest SST appeared in the southeastern part of the East China Sea. In summer and autumn, SST was high and relatively spatially homogeneous compared to that in winter and spring with a range of ~18 to 30°C. Monthly variability of the SST illustrated the lowest appeared in January to March and the highest in July to September (Guo et al. 2015). Arora et al. (2016) found that although SST in the tropical Indian Ocean has continued to increase, SST in the tropical Pacific has shown a cooling trend in the last decades (2002-2012). It is a well known fact that the Indian Ocean and Pacific Ocean are very strongly coupled to each other and the warming of the vast Indian Ocean basin is triggered by El Niño on interannual time scales. However, in the last decade, this relationship has weakened. Recent Indian Ocean warming is triggering a Matsuno-Gill type response in the atmosphere by producing anomalous cyclonic circulation on both sides of the equator over the tropical Indian Ocean and eastward anomalies along the tropical Pacific Ocean.

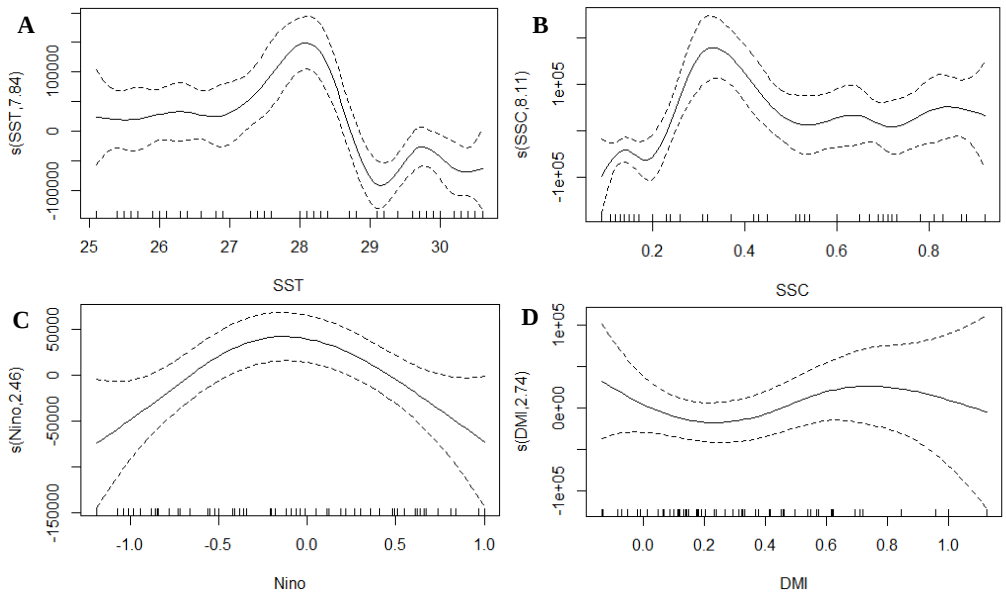

Figure 11. GAM Plot: A. SST, B. Chlorophyll-a (SSC), C. Nino 3.4; D. DMI

During 5 recent years, the highest chlorophyll-a concentration value was found in August. However, in 2021 the peak of chlorophyll-a retreated to transitional season 2, namely in September. Then chlorophyll-a decreased starting from the end of the transition season 2, the west season, until the beginning of the transition season 1. The highest annual average of chlorophyll-a was in September with a value of 0.76 mg/m^3. The lowest annual average of chlorophyll-a was in January, with a value of 0.12 mg/m^3. In June-August (east season), the average chlorophyll-a tend to be high until its peak in September - November (transition season 2). On the other hand, in the western season, the value of chlorophyll-a concentration decreases. Partial analysis on the existence of small pelagic fish with the chlorophyll-a concentration found a close relationship of 69.66%. It also revealed that the lowest catch was found at the chlorophyll-a concentration lower than 0.2 mg/m^3 (Tangke and Senen 2020).

The upwelling phenomenon is closely related to the concentration of chlorophyll-a in the waters. When the El Nino phase ENSO phenomenon occurs, the upwelling in the waters south of Java increases. The upwelling phenomenon thus affect the SST to decrease while there is increase in chlorophyll-a concentration. The opposite occur in the La Nina phase of the ENSO phenomenon. The exact impact also appears in the IOD phenomenon in the negative IOD phase, upwelling weakens and affect the SST to increase resulting in the decrease in concentration of chlorophyll-a. The opposite happens when the IOD phenomenon in the positive IOD phase. The occurrence of upwelling indirectly affects the productivity of the fish caught. The study of Atmadipoera et al. (2018) in the Maluku Sea illustrated that the upwelling is mainly forced by fully developed southerly monsoon winds, dragging surface water northward like the wind direction since the effect of Coriolis vanishes near the equator. The upwelling occurs during the Southeast Monsoon period from June to October, and reach maximum in September. Warm surface water in the center upwelling is replaced by upwelled colder water from about 60 m, which evolves from southern to northern region then curving to northeastern due to the boundary of Sulawesi mainland (Atmadipoera et al. 2018).

The GAM plot (Figure 11) shows that if the line in the plot is above the value 0, the effect is more substantial. Conversely, when the line on the plot is below the value 0, the effect is weaker. Low SST and high chlorophyll-a concentrations significantly affect the productivity of yellowfin tuna. Under normal conditions, Nino 3.4 also affects the productivity of larger fish. Meanwhile, the GAM plot on the DMI variable did not show a significant increase in the response variable. However, fish productivity increases slightly in the range < 0.0°C and 0.4°C-1°C.

The best model from the GAM analysis was the combination of chlorophyll-a and nino 3.4 or the ENSO phenomenon. Table 3 also shows oceanographic conditions in waters such as SST and chlorophyll-a affect fish catches. According to Saputra et al. (2017), the El Nino Southern Oscillation phenomenon was followed by fluctuating catches caused by the correlation between El-Nino and La-Nina phenomena with the concentration of chlorophyll-a in the waters. Chlorophyll-a in water is a food source for phytoplankton. The fertility of a waters can be measured or determined by looking at the water's chlorophyll-a concentration. The concentration of chlorophyll-a indirectly affects yellowfin tuna due to the food chain process. The food chain plays an important role in the marine ecosystem, where chlorophyll-a, the green pigment in phytoplankton, is proportional to the phytoplankton's biomass. Phytoplankton are in turn consumed by zooplankton, which are then consumed by small fish. These small fish become prey for larger fish, including large pelagic fish such as yellowfin tuna. Fraile et al. (2010) reported that chlorophyll-a has a positive relationship with skipjack abundance; the higher the chlorophyll concentration is, more skipjack tuna is present. In contrast, depth of thermocline is inversely related to skipjack abundance. Kumar et al. (2014) in the study on tuna fisheries described that the ENSO impact on climate, tuna abundance, distribution of habitats, and tuna catch in the Indian Ocean. Generalized Additive Models shows that the parameter of SST explained the highest deviance, and it is regarded as the best predictor of tuna habitat in the Indian Ocean, followed by sea level pressure and winds.

The results of fishing operations are not only affected by chlorophyll-a, but also by wind conditions and fishing habits. During the westerly season, which typically lasts from October to February, there are high waves, storms, strong winds, and extreme weather. The famine season, characterised by west winds, leads to fishermen not getting catches commensurate with the cost of going to sea or losing money. On the other hand, during the east monsoon, the wind direction is mostly oriented towards the southeast. This season's weather conditions tend to be relatively good due to the weakening intensity of rainfall. The famine season causes the number of fishermen's catches to decrease. In the harvest season (east wind), fishermen can go to sea 1-2 times a day. However, catches tend to decrease during westerly winds caused by large wave conditions, which cause fish to swim away. The increase in fish catch due to high chlorophyll-a concentrations takes time because of the energy transfer process in a food chain (Sartimbul et al. 2010).

In conclusion, the study aimed to determine the effect of climate anomalies on the productivity of yellowfin tuna in the Indian Ocean south of East Java. The study confirmed that fish abundance and migration are influenced by oceanographic factors, including annual and interanual variations of climatic factors. SST in the study area tend to decrease in the east monsoon, while the average of chlorophyll-a tend to be high in the east monsoon. The phenomenon of climate anomalies during 2017-2021 according to the ENSO index value (Nino 3.4) and the IOD index value (DMI) obtained 3 ENSO and 3 IOD phenomena. The anomaly of oceanography factors tend to be positive in the El Nino phenomenon and tend to have a negative value in the period of La Nina phenomenon. When a weak La Nina phenomenon occurred in 2017-2018 for a period of 7 months (September-March) the catch of

yellowfin tuna decreased. GAM analysis showed that the best model combines chlorophyll-a + Nino 3.4. Oceanographic parameters, SST and chlorophyll-a variables in the model also showed a significant effect on fish catch. The results of the Pearson correlation analysis showed that the ENSO phenomenon was not influenced by SST or chlorophyll-a. On the other hand, SST and chlorophyll-a had a significant effect on the IOD phenomenon with low correlation. The study contributed an approach for the assessing fish abundance and migration using the analysis of oceanographic and cline phenomena in the spatial and temporal perspective for the sustainable management of yellowfin tuna catches.

ACKNOWLEDGEMENTS

The authors thank Pondokdadap Fishing Port Sendang Biru, Malang, East Java, Indonesia, for collecting fisheries data. Thanks to NASA also for providing ocean color data, Nino 3.4, and DMI data. This research was funded by the Institute of Research and Community Services Universitas Brawijaya, Indonesia, under the *Hibah Penelitian Utama* 2022 scheme.

REFERENCES

Amri K, Satria F. 2013. Impact of climate anomaly on catch composition of neritic tuna in Sunda Strait. Indones Fish Res J 19 (2): 61-72. DOI: 10.15578/ifrj.19.2.2013.61-72.

Aranda G, Abascal FJ, Varela JL, Medina A. 2013. Spawning behaviour and post-spawning migration patterns of atlantic bluefin tuna (*Thunnus thynnus*) ascertained from satellite archival tags. PLoS One 8 (10): e76445. DOI: 10.1371/journal.pone.0076445.

Arora A, Rao SA, Chattopadhyay R, Goswami T, George G, Sabeerali CT. 2016. Role of Indian Ocean SST variability on the recent global warming hiatus. Glob Planet Change 143: 21-30. DOI: 10.1016/j.gloplacha.2016.05.009.

Atmadipoera AS, Khairunnisa Z, Kusuma DW. 2018. Upwelling characteristics during El Nino 2015 in Maluku Sea. IOP Conf Ser: Earth Environ Sci 176: 012018. DOI: 10.1088/1755-1315/176/1/012018.

Barnston AG, Tippett MK, L'Heureux ML, Li S, DeWitt DG. 2012. Skill of real-time seasonal ENSO model predictions during 2002-11: Is our capability increasing? Bull Am Meteorol Soc 93 (5): 631-651. DOI: 10.1175/BAMS-D-11-00111.2.

Bjerknes JA. 1966. A possible response of the atmospheric Hadley circulation to equatorial anomalies of ocean temperature. Tellus 18 (4): 820-829. DOI: 10.3402/tellusa.v18i4.9712.

Cadrin SX, Dickey-Collas M. 2014. Stock assessment methods for sustainable fisheries. ICES J Mar Sci 72 (1): 1-6. DOI: 10.1093/icesjms/fsu228.

Fadlan A, Sugianto DN, Kunarso, Zainuri M. 2017. Influence of ENSO and IOD to variability of sea surface height in the north and south of Java Island. IOP Conf Ser: Earth Environ Sci 55: 012021. DOI: 10.1088/1755-1315/55/1/012021.

Fonteneau A, Pereira JG. 2012. Analysis of the daily catch and effort data of the bluefin (*Thunnus thynnus*) Algarve trap fishery during the years 1898-1900. Aquat Living Resour 25 (4): 297-310. DOI: 10.1051/alr/2012023.

Fraile I, Murua H, Goñi N, Caballero A. 2010. Effects of environmental factors on catch rates of FAD-associated yellowfin (*Thunnus albacares*) and skipjack (*Katsuwonus pelamis*) tunas in the western Indian Ocean. Indian Ocean Tuna Commission Proceedings, 22. IOTC-2010-WPTT-46.

George G, Jayaraman J, Shah P, Joseph T, Raj MS, Shafeeque M, Platt T, Sathyendranath S. 2019. How oceanography influences fishery biology? - A case of distribution differences in carnivorous and planktivorous fishes along the Coastal Waters of Eastern Arabian Sea. In: Recent Advances in Fishery Biology Techniques for Biodiversity Evaluation and Conservation. Central Marine Fisheries Research Institute, Kochi, Kerala.

George G. 2014. Numerical modelling and satellite remote sensing as tools for research and management of marine fishery resources in remote sensing and modeling: advances in coastal and marine resources. In: Finkl C, Makowski C (Eds). Remote Sensing and Modeling. Springer International Publishing, Switzerland. DOI: 10.1007/978-3-319-06326-3_18.

Guo XH, Zhai WD, Dai MH, Zhang C, Bai Y, Xu Y, Li Q, Wang GZ. 2015. Air-sea CO_2 fluxes in the East China Sea based on multiple-year underway observations. Biogeosciences 12 (18): 5495-5514. DOI: 10.5194/bg-12-5495-2015.

Harlyan LI, Sambah AB, Iranawati F, Ekawaty R. 2020. Klasterisasi spasial keragaman spesies tuna di perairan Selatan Jawa. Jurnal Perikanan Universitas Gadjah Mada 23 (1): 9-16. DOI: 10.22146/jfs.58917. [Indonesian]

Hsu TY, Chang Y, Lee MA, Wu RF, Hsiao SC. 2021. Predicting skipjack tuna fishing grounds in the western and central pacific ocean based on high-spatial-temporal-resolution satellite data. Remote Sens 13 (5): 861. DOI: 10.3390/rs13050861.

Kratzer S, Alikas K, Harvey T, Beltrán-Abaunza JM, Morozov E, Mustapha SB, Lavender S. 2016. Multitemporal remote sensing of coastal waters. In: Ban Y (eds). Multitemporal Remote Sensing. Remote Sensing and Digital Image Processing. Springer, Cham. DOI: 10.1007/978-3-319-47037-5_19.

Kumar PS, Pillai GN, Manjusha U. 2014. El Nino Southern Oscillation (ENSO) impact on tuna fisheries in Indian Ocean. Springerplus 3 (1): 591. DOI: 10.1186/2193-1801-3-591.

Lau KM, Yang S. 2022. Walker Circulation In: Holton J, Pyle JP, Curry J (eds). Encyclopedia of atmospheric sciences. Academic Press, London.

Lee MZ, Mekanik F, Talei A. 2022. Dynamic neuro-fuzzy systems for forecasting El Niño Southern Oscillation (ENSO) using oceanic and continental climate parameters as inputs. J Mar Sci Eng 10 (8): 1161. DOI: 10.3390/jmse10081161.

Lira CP, Taborda R. 2014. Advances in applied remote sensing to coastal environments using free satellite imagery. In: Advances in Coastal and Marine Resources: Remote Sensing and Modeling. Edition: Coastal Research Library Chapter 4. Springer International Publishing, Switzerland. DOI: 10.1007/978-3-319-06326-3_4.

Lumban-Gaol J, Leben RR, Vignudelli S, Mahapatra K, Okada Y, Nababan B, Mei-Ling M, Amri K, Arhatin RE, Syahdan M. 2015. Variability of satellite-derived sea surface height anomaly, and its relationship with bigeye tuna (*Thunnus obesus*) catch in the Eastern Indian Ocean. Eur J Remote Sens 48 (1): 465-477. DOI: 10.5721/EuJRS20154826.

Monolisha S, Platt T, Sathyendranath S, Jayasankar J, George G, Jackson T. 2018. Optical classification of the coastal waters of the Northern Indian Ocean. Front Mar Sci 5: 87. DOI: 10.3389/fmars.2018.00087.

Mugo R, Saitoh SI, Nihira A, Kuroyama T. 2010. Habitat characteristics of skipjack tuna (*Katsuwonus pelamis*) in the Western North Pacific: A remote sensing perspective. Fish Oceanogr 19 (5): 382-396. DOI: 10.1111/j.1365-2419.2010.00552.x.

NOAA ESRL Physical Sciences Laboratory. 2018. Niño 3.4 SST Index. Updated: Jul 31, 2018. National Oceanic and Atmospheric Administration. https://psl.noaa.gov/gcos_wgsp/Timeseries/Nino34/.

Novitasari F, Nelwan AP, Farhum SA. 2022. Musim penangkapan ikan tuna sirip kuning (*Thunus albacares*) menggunakan alat tangkap pancing ulur di perairan Teluk Bone yang didaratkan di Kabupaten Luwu. Jurnal Penelitian Perikanan Indonesia 28 (1): 1-17. DOI: 10.15578/jppi.28.1.2022.1-6. [Indonesian]

Nur'utami MN, Hidayat R. 2016. Influences of IOD and ENSO to Indonesian rainfall variability: Role of atmosphere-ocean interaction in the indo-pacific sector. Procedia Environ Sci 33: 196-203. DOI: 10.1016/j.proenv.2016.03.070.

Pauly D, Zeller D. 2016. Catch reconstructions reveal that global marine fisheries catches are higher than reported and declining. Nat Commun 7: 10244. DOI: 10.1038/ncomms10244.

Peck MA, Baumann H, Bernreuther M, Clemmesen C, Herrmann JP, Haslob H, Huwer B, Kanstinger P, Köster FW, Petereit C, Temming A, Voss R. 2012. The ecophysiology of *Sprattus sprattus* in the Baltic and North Seas. Prog Oceanogr 103: 42-57. DOI: 10.1016/j.pocean.2012.04.013.

Peck MA, Reglero P, Takahashi M, Catalán IA. 2013. Life cycle ecophysiology of small pelagic fish and climate-driven changes in

populations. Prog Oceanogr 116: 220-245. DOI: 10.1016/j.pocean.2013.05.012.

Ren HL, Jin FF, Song LC, Lu B, Tian B, Zuo J, Liu Y, Wu J, Zhao C, Nie Y, Zhang P, Ba J, Wu Y, Wan J, Yan Y, Zhou F. 2017. Prediction of primary climate variability modes in Beijing Climate Center. J Meteorol Res 31: 204-223. DOI: 10.1007/s13351-017-6097-3.

Ren HL, Zuo J, Deng Y. 2019. Statistical predictability of Niño indices for two types of ENSO. Clim Dyn 52: 5361-5382. DOI: 10.1007/s00382-018-4453-3.

Sambah AB, Miura F, Kadarisman HP, Sartimbul A. 2013. Remote sensing application for *Sardinella lemuru* assessment: A case study of the south Waters of Malang Regency, East Java, Indonesia. In: Frouin RJ, Ebuchi N, Pan D, Saino T (eds). Remote Sen Mar Environ II Proc SPIE, Bellingham, 2013. DOI: 10.1117/12.976284.

Santoso A, Mcphaden MJ, Cai W. 2017. The defining characteristics of ENSO extremes and the strong 2015/2016 El Niño. Rev Geophys 55 (4): 1079-1129. DOI: 10.1002/2017RG000560.

Santoso TW, Kunarso, Marwoto J. 2021. Analisa spasial dan temporal suhu permukaan laut dan klorofil-a selama 2 dekade di perairan Indonesia. Indones J Oceanogr 3 (4): 370-381. DOI: 10.14710/ijoce.v3i4.12384. [Indonesian]

Saputra C, Arthana IW, Hedrawan IG. 2017. Studi ancaman sumber daya ikan lemuru (*Sardinella lemuru*) di Selat Bali hubungannya dengan ENSO dan IOD. Ecotrophic Jurnal Ilmu Lingkungan 11 (2): 140-147. [Indonesian].

Sari QW, Utari PA, Setiabudidaya D, Yustian I, Siswanto E, Iskandar I. 2020. Surface chlorophyll-a variations in the Southeastern Tropical Indian Ocean during various types of the positive Indian Ocean Dipole events. Intl J Remote Sens 41 (1): 171-184. DOI: 10.1080/01431161.2019.1637962.

Sartimbul A, Nakata H, Rohadi E, Yusuf B, Kadarisman HP. 2010. Variations in chlorophyll-a concentration and the impact on *Sardinella lemuru* catches in Bali strait, Indonesia. Prog Oceanogr 87 (1-4): 168-174. DOI: 10.1016/j.pocean.2010.09.002.

Setiawati MD, Sambah AB, Miura F, Tanaka T, As-syakur AR. 2015. Characterization of bigeye tuna habitat in the Southern Waters off Java-Bali using remote sensing data. Adv Space Res 55 (2): 732-746. DOI: 10.1016/j.asr.2014.10.007.

Setyadji B, Amri K. 2017. Pengaruh anomali iklim (ENSO dan IOD) terhadap sebaran ikan pedang (*Xiphias gladius*) di Samudera Hindia bagian timur. Jurnal Segara 13 (1): 49-63. DOI: 10.15578/segara.v13i1.6422. [Indonesian]

Simanjuntak F, Lin TH. 2022. Monsoon effects on chlorophyll-a, sea surface temperature, and ekman dynamics variability along the southern coast of lesser Sunda islands and its relation to ENSO and IOD based on satellite observations. Remote Sens 14 (7): 1682. DOI: 10.3390/rs14071682.

Sprintall J, Revelard A. 2014. The Indonesian throughflow response to Indo-Pacific climate variability. J Geophys Res: Ocean 119 (2): 1161-1175. DOI: 10.1002/2013JC009533.

Syamsuddin ML, Saitoh SI, Hirawake T, Bachri S, Harto AB. 2013. Effects of El Niño-Southern oscillation events on catches of bigeye tuna (*Thunnus obesus*) in the eastern Indian Ocean off Java. Fish Bull 111 (2): 175-188. DOI: 10.7755/FB.111.2.5.

Tangke U, Senen B. 2020. Distribution of sea surface temperature and chlorophyll-a concentration its correlation with small pelagic fish catch in Dodinga Bay. IOP Conf Ser: Earth Environ Sci 584: 012020. DOI: 10.1088/1755-1315/584/1/012020.

Thushara V, Vinayachandran PN. 2020. Unprecedented surface chlorophyll blooms in the Southeastern Arabian Sea during an extreme negative Indian Ocean Dipole. Geophys Res Lett 47 (13): e2019GL085026. DOI: 10.1029/2019GL085026.

Wang C, Deser C, Yu JY, DiNezio P, Clement A. 2017. El Niño and Southern Oscillation (ENSO): A review. In: Glymn P, Manzello D, Enochs I. Coral Reefs of the Eastern Pacific (Eds). Springer Science Publisher, Dordrecht. DOI: 10.1007/978-94-017-7499-4_4.

Wijaya A, Zakiyah U, Sambah AB, Setyohadi D. 2020. Spatio-temporal variability of temperature and chlorophyll-a concentration of sea surface in Bali Strait, Indonesia. Biodiversitas 21 (11): 5283-5290. DOI: 10.13057/biodiv/d211132.

Yang G, Zhao X, Li Y, Liu L, Wang F, Yu W. 2019. Chlorophyll variability induced by mesoscale eddies in the southeastern tropical Indian Ocean. J Mar Syst 199: 103209. DOI: 10.1016/j.jmarsys.2019.103209.

Zhang T, Song L, Yuan H, Song B, Ngando NE. 2021. Comparative study on habitat models for adult bigeye tuna in the Indian Ocean based on gridded tuna longline fishery data. Fish Oceanogr 30 (5): 584-607. DOI: 10.1111/fog.12539.